

Continual Learning for Instruction Following from Realtime Feedback

Alane Suhr
Allen Institute for AI*
alanes@allenai.org

Yoav Artzi
Cornell University
yoav@cs.cornell.edu

Abstract

We study the problem of continually training an instruction-following agent from feedback provided by users during collaborative interactions. During interaction, human users instruct an agent using natural language, and provide realtime binary feedback as they observe the agent’s instruction execution. We cast learning as a contextual bandit problem, converting the user feedback to immediate reward. We evaluate through multiple rounds of human-agent interactions, demonstrating 15.4% absolute improvement in instruction execution over time. We also show our approach is robust to several design variations, and that the feedback signal is roughly equivalent to the learning signal of supervised demonstration data.

1 Introduction

The dynamics that arise in situated language interactions between human users and automated agents expose a plethora of language learning signals. A prime example of such a signal is explicit feedback: when users convey their intent via natural language instructions for an agent to follow, they are well positioned to provide feedback, for example, through a stream of binary signals as the agent acts.

Learning from this type of signal has significant potential. It shifts the burden of learning from annotated data to learning through interaction with users, which not only reduces data costs, but also enables continual improvement through interaction with users. This signal also fundamentally differs from gold-standard annotated data: it directly targets current agent behavior, rather than reflecting optimal human behavior that may be of less relevance to the agent’s current policy. This approach stands in contrast with most methods for learning to follow instructions, where the use of demonstration data entails high data costs, and the clear separation between training and deployment passes over

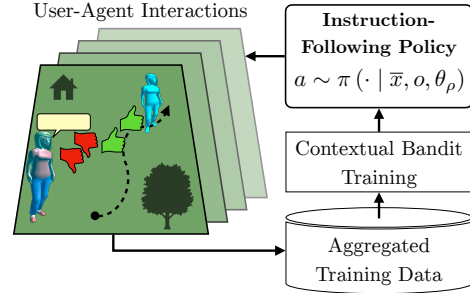


Figure 1: Illustration of our continual learning process. We iterate between deployment and training. In each round, during deployment, we sample and execute actions conditioned on user-written instructions, while users provide binary feedback as they observe instruction execution. We train each subsequent policy using a contextual bandit objective using the feedback data.

opportunities for learning through interaction with users (e.g., Artzi and Zettlemoyer, 2013; Anderson et al., 2018; Shridhar et al., 2020).

In this paper, we study the problem of continually improving an automated instruction-following agent¹ by learning from user feedback in human-agent interactions. We situate the interaction in a collaborative environment, which provides conditions necessary for this type of learning: users are incentivized to improve the agent’s capabilities by providing feedback, and are continuously present as the agent executes their instructions. We use the CEREALBAR scenario (Suhr et al., 2019), where two participants collaborate towards a common goal in a shared world, using natural language instructions to coordinate their actions. During interaction, human users write instructions for an agent, and provide feedback to the agent as it executes them via a stream of binary signals. Figure 1 illustrates the setup and our learning process.

A key challenge is the complexity of the learning signal. Users provide feedback at their discretion and under time pressure as the agent executes their

*Work done while at Cornell University.

¹Throughout the paper, we use *agent* to refer to an automated instruction-following system.

instructions. This results in an unpredictable, and often noisy, learning signal. While the concurrency of agent actions and user feedback provides a form of weak alignment, delays in human response and the lack of clarity about which action or actions they critique make attributing the learning signal to specific actions challenging. Further complicating learning is the feedback loop created by the continually changing agent behavior and constant adaptation by human users. These factors create a scenario that is particularly difficult for complex, even if expressive methods, as they often make various assumptions about the learning signal and the interaction dynamics (Knox and Stone, 2009; MacGlashan et al., 2017). We opt for a simple approach with minimal assumptions and formulate learning as a contextual bandit scenario. We alternate between deployment, where the agent interacts with users that provide feedback, and training, where we compute immediate rewards from feedback signals, and weigh examples using the current policy to account for the continually changing agent behavior.

We experiment with our approach through interactions with human users, where we repeatedly deploy, train, and re-deploy the agent. We study the effects of human adaptation and process design decisions on the efficacy of learning. We design our experiments to tease apart genuine agent improvements from human user adaptation, and observe dramatic improvements in agent behavior beyond what user adaptation explains, 15.4% absolute improvement in instruction execution accuracy in our longer running experiment. Our code and data will be released upon publication.

2 Technical Overview

Interaction Scenario We situate user-agent interactions in CEREALBAR (Suhr et al., 2019), a collaborative scenario where two participants, a leader and a follower, collect sets of matching cards together in a shared, 3D environment. The two participants collaborate towards a shared goal (i.e., completing sets of cards), act in the world, and coordinate using natural language. The leader plans what the pair should do, acts according to the plan, and describes the follower’s part of the plan using natural language instructions. The follower’s role is to follow the instructions. The pair receives a point for each set of cards they successfully collect. Their goal is to maximize their score. We add to the original CEREALBAR setting the ability for the

leader to provide binary feedback signals to the follower as they execute instructions. In our study, the agent controls the follower and the leader is always a human user.

Task The agent’s task is to map natural language instructions and observations to follower actions. Actions include moving FORWARD or BACKWARD, turning LEFT or RIGHT, and completing instruction execution with STOP. The agent observation is a partial view of the world state from the first-person perspective of the follower. Formally,² given an instruction \bar{x} and an initial observation o_1 , our goal is to generate a sequence $\langle (o_1, a_1), \dots, (o_m, a_m) \rangle$, where o_i an agent observation, a_i is the action taken, and $a_m = \text{STOP}$.

Inference and Learning We define the follower agent as a policy $\pi(\bar{x}, o; \theta)$ parameterized by θ that maps instructions \bar{x} and state observations o to a distribution over actions. During interaction with users, for each user-written instruction \bar{x} , we sample and execute actions $a_i \sim \pi(\cdot \mid \bar{x}, o_i; \theta)$ until we sample the instruction completion action. Concurrently, the user may provide positive and negative feedback signals f . Feedback signals are given in realtime, and are not timed to coincide with a specific action. Between any two agent steps, there could be any number of feedback signals. We optimize parameters through rounds of continual learning (Figure 1). The execution of an instruction \bar{x} during interaction creates a trace made of two sequences $(\langle (o_i, a_i, w_i^a) \rangle_{i=1}^m, \langle (f_j, w_j^f) \rangle_{j=1}^n)$, where each action a_i and feedback signal f_j are paired with wall time w_i^a or w_j^f . At each round ρ , we deploy the policy with parameters θ_ρ to interact with users, and then estimate parameters $\theta_{\rho+1}$. During deployment, we collect agent instruction execution and user feedback. We compute reward from the feedback to construct training examples (\bar{x}, o, a, r) , where r is a reward. We optimize the policy parameters at each round by solving a contextual bandit problem, maximizing immediate expected reward.

Evaluation Our main metric is instruction execution accuracy for user-written instructions. Because we have no access to ground-truth demonstrations, but only to executions of our agent, we cannot compute accuracy automatically. We instead use acquire human judgments of follower accuracy after

²Suhr et al. (2019) provide complete formal notation for CEREALBAR. We use a simplified notation to focus on the follower instruction following task only.

each round of deployment through separate crowdsourcing. We also evaluate performance through trends in user feedback and ratings over time.

3 Continual Learning

We estimate the policy parameters from user feedback during interaction with users. The processes progress in rounds. Each round ρ includes: (a) deploying the agent policy parameterized by θ_ρ to interact with users (Section 3.1), (b) computing rewards from user feedback to construct training data \mathcal{D}_ρ (Section 3.2), and (c) optimizing the policy parameters using all data observed so far $\bigcup_{\rho'=0}^{\rho} \mathcal{D}_{\rho'}$ to compute $\theta_{\rho+1}$ (Section 3.3). We initialize the process with a policy parameterized by θ_1 estimated on human demonstration data \mathcal{D}_0 .

3.1 Deployment Interactions

During deployment in round ρ , users collaborate with the agent, and delegate to it tasks by typing natural language instructions. For each instruction \bar{x} , we sample a sequence of actions from the policy $a_i \sim \pi(\cdot | \bar{x}, o_i; \theta_\rho)$. Executing an action in the environment results in a new observation o_{i+1} . For each action, we record the wall time w_i^a as the time when the user starts seeing the follower starting to execute the action (i.e., the action animation starts). We terminate instruction execution when the stop action STOP is sampled.

At any point during the agent instruction execution, the user may provide binary (positive or negative) feedback signals, creating a stream $\langle (f_j, w_j^f) \rangle_{j=1}^n$ where w_j^f is the user's wall time when a feedback button is pressed. We also allow the user to manually reboot the follower at any point during an instruction execution. This is meant to terminate very bad executions before they damage the interaction too much, for example by leading the follower astray too far. Rebooting adds a negative feedback signal to the end of the stream, and removes all queued instructions.³

The execution of an instruction by the agent and the feedback given by the user are combined together to create an trace made of two sequences $\langle (o_i, a_i, w_i^a) \rangle_{i=1}^m, \langle (f_j, w_j^f) \rangle_{j=1}^n$.

3.2 Dataset Construction

We use all traces collected in round ρ to construct a training dataset \mathcal{D}_ρ . Each example in \mathcal{D}_ρ is a

³CEREALBAR allows the leader to queue multiple instructions for the follower to execute. The follower only sees the current instruction.

tuple (\bar{x}, o, a, r) , where \bar{x} is an instruction written by the user in round ρ , o is the agent observation when action a was selected during the execution \bar{x} in the interaction, and r is a numerical reward we compute from the feedback stream. For each instruction written during round ρ we may create no examples if no feedback was given, or multiple examples if computing the rewards from feedback resulted in attributing rewards to multiple actions.

Simple Reward We consider the value of each positive feedback as $f = +1$ and each negative feedback as $f = -1$. We compute the reward r_i for an action a_i as the sign of sum of feedback signals that occur between it and the next action after correcting for human response delay time (MacGlashan et al., 2017):

$$r_i = \text{sgn} \sum \left\{ f_j \mid w_i^a < w_j^f - d \leq w_{i+1}^a \right\}, \quad (1)$$

where w_i^a is the wall time of action a_i , w_j^f is the wall time of feedback signal f_j , and d is a human response delay constant, which we set to 0.2 seconds. If the set is empty because there are no feedback signals within the time window, or if $r_i = 0$, we do not set a reward or create an example for the corresponding action.

Heuristically Propagated Reward The simple reward computation is likely to result in relatively sparse reward assignment, with many actions not receiving any learning signal. This is because users are not required to follow any particular feedback schedule. Indeed, in our experiments, we observe that roughly only 63.1% of actions receive feedback. However, human feedback may not be about the most recent action only, but can potentially be attributed to multiple recent actions. For example, the user may not be certain if to discourage a behavior, such as turning and going in a certain direction, until the trajectory is clear after several steps.

We address this by taking inspiration from the use of eligibility traces for credit assignment (Sutton and Barto, 1998), and create heuristics to propagate the reward to actions that otherwise receive no reward. If an action is assigned no reward, we propagate to it a reward from a later action by assigning to it the reward of the next action that is assigned one, if one exists within the next eight actions. The only exception is that we do not propagate reward from a STOP action that receives a negative reward.

We additionally prevent noisy feedback from being propagated by considering the scenario dynam-

ics. We remove all training examples for actions following an action that results in card interaction (i.e., selecting or de-selecting a card) that receives a negative reward. If an action results in an invalid set (i.e., the cards selected cannot make a valid set), we remove it from the training data and do not propagate its award. These scenario-specific heuristics were developed by identifying common feedback errors in the data. Following propagation, we observe that 82.2% of the actions have reward assigned to them, up from 63.1, without increasing the reward error rate of about 7.0.⁴

3.3 Parameter Optimization

We use a contextual bandit policy gradient objective to maximize the expected immediate reward (Misra et al., 2017). At the end of each round, we train from scratch using all the data observed so far $\bigcup_{\rho'=0}^{\rho} \mathcal{D}_{\rho'}$. We process the initial human demonstration data \mathcal{D}_0 to the same form as the reward data we get from user interactions, so we can use it seamlessly with the data we get from the rounds. For each action a and input instruction \bar{x} and observation o in \mathcal{D}_0 , we create an example $(\bar{x}, o, a, +1)$ by setting the action reward to +1.

During round ρ , the gradient for an example (\bar{x}, o, a, r) from dataset \mathcal{D}'_{ρ} , $\rho' \leq \rho$ is:

$$\begin{aligned} \nabla \mathcal{L}_{\theta} &= c(a, \bar{x}, o, \rho') r \nabla \log \pi(a | \bar{x}, o; \theta) \quad (2) \\ c(a, \bar{x}, o, \rho') &= \begin{cases} \min \left(1, \frac{\pi(a | \bar{x}, o; \theta)}{\pi(a | \bar{x}, o; \theta_{\rho'})} \right) & \rho' > 0 \\ 1 & \rho' = 0 \end{cases}, \end{aligned}$$

where $c(\cdot)$ computes a clipped inverse propensity scoring (IPS) coefficient of the policy gradient (Horvitz and Thompson, 1952), and $\theta_{\rho'}$ are parameters with which the examples in $\mathcal{D}_{\rho'}$ were generated. IPS is commonly used for debiasing policies during off-policy learning. We also use IPS to avoid the problem of exploding gradients while training on negative examples ($r < 0$) (Kojima et al., 2021). We clip the value of the IPS coefficient to a maximum of 1 to avoid overfitting on positive examples (Gao et al., 2022). We perform gradient updates across batches of training examples. We update parameters with $\theta \leftarrow \theta + \mu \text{ADAM}(\mathbb{E}(\nabla \mathcal{L}_{\theta}))$, where μ is the learning rate and \mathbb{E} computes an expectation of the gradient using items in a training batch.

⁴Error rate is determined via a qualitative analysis of 100 randomly-sampled instructions.

4 Experimental Setup

Initialization Data Except when specified otherwise, the demonstration training dataset \mathcal{D}_0 includes 8,790 instructions from 456 randomly-sampled human-human interactions from Suhr et al. (2019). Pilots studies showed estimating θ_1 using this data provides a good balance of human-human data amount and initial system performance for interaction with human users.

Model We implement the policy π as a neural network with parameters θ . Roughly, the instruction \bar{x} and observation o are embedded independently. The representation of o is similar to that of Suhr et al. (2019), but accounts for partial observability. We perform instruction-conditioned convolutions on the embedded observation to mix features from both inputs, and use a modified LINGUNET (Blukis et al., 2018b) to generate a distribution over actions. Appendix A provides formal model details.

Deployment In each round of deployment, we collect up to a fixed number of interactions per user. We instruct users to use the reboot button sparingly, and only when they anticipate the follower will make a mistake that cannot be easily corrected. We do not enforce any specific feedback patterns. Users are aware that their instructions and feedback will be used to train the agent for future rounds.

Evaluation The main measure of performance is the agent’s instruction execution accuracy during interactions with human users. Because we have no human demonstration or annotation for this data, we perform post-hoc manual evaluation for each round. We randomly sample instructions from each round. We only sample instructions the agent completed (i.e., executed the STOP action) to annotate. We assume all instructions rebooted by the user are failures, and adjust down the accuracy as estimated from the annotations according to the ratio of rebooted instructions.⁵ We show the instruction, an animation of the agent’s execution, and a list of cards that were reached by the follower during execution. We ask whether the follower correctly executed the instruction, and whether the follower made any number of errors in a pre-defined list. For performance measurements and statistics, we report the mean and confidence interval,⁶ except

⁵Appendix C formally defines the evaluation metric.

⁶Confidence intervals are computed using bootstrap sampling. $n = 10,000$ samples for interaction-level metrics, and n

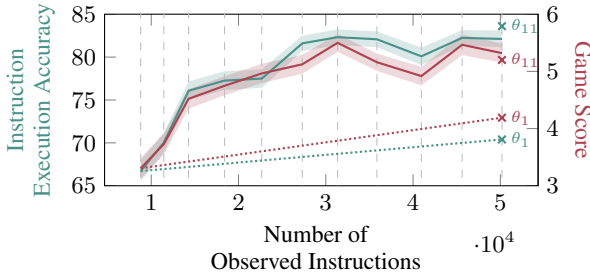


Figure 2: Mean estimated instruction execution accuracy and game scores across 11 rounds. The x-axis shows the number of instructions observed. Dashed lines show round boundaries. We mark with \times the accuracies and scores from the post-hoc study of user adaptation for θ_1 and θ_{11} . The dotted lines illustrate the share of the improvement due to user adaptation.

where noted. When emphasizing the relationship between the amount of training data and each measure, we plot the metric by the number of observed instructions rather than by round index.

Crowdsourcing We use MTurk⁷ for both user-agent interactions and post-hoc instruction evaluation. We recruit workers from English-majority locales using a qualification quiz and tutorial.⁸ We maintain novice and expert groups of workers. Expert workers have higher compensation, and access to the post-hoc instruction accuracy tasks. To become an expert, workers must show they understand the task and annotation expectations during interactions in the novice pool. We qualify 108 workers, including 65 expert workers. During deployment, we balance the number of interactions between workers by limiting each worker to about eight interactions per agent and round.

5 Results and Analysis

We conduct two experiments: an 11-round experiment to observe long-term learning and user behavior trends, and a shorter 5-round experiment to compare several learning design decisions.

5.1 Long-Term Experiment

We evaluate over eleven rounds of deployment and training. This experiment uses the heuristically propagated reward, with the goal of obtaining more training examples compared to the simple reward (Section 3.2). In total, we collect 3,368 games and 46,573 instructions, at a cost of \$15,944.45 USD.

⁷ = 1,000 samples for instruction- and action-level metrics.

⁸<https://www.mturk.com>

⁹Details about crowdsourcing management and compensation are available in Appendix D.

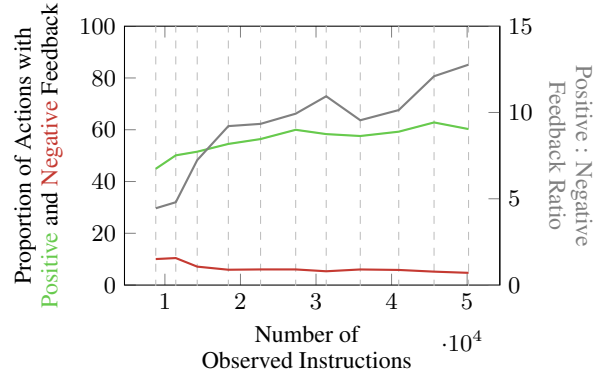


Figure 3: Proportion of actions receiving positive and negative feedback from users over 11 rounds, and the ratio of frequency between positive and negative feedback. The x-axis shows the number of instructions observed. Dashed lines show round boundaries.

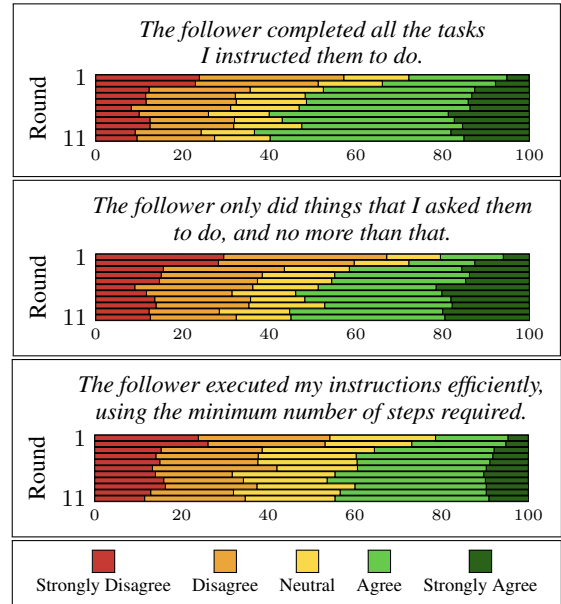


Figure 4: Distribution of post-interaction user agreement with three statements about agent performance.

Agent Accuracy Figure 2 shows estimated instruction execution accuracy and number of points across the eleven rounds. Accuracy improves from 66.7 ± 1.5 in the initial round to 82.1 ± 1.1 in the final round.⁹ The continual learning process also results in increased interaction success: the game score increases from 3.3 ± 0.2 to 5.3 ± 0.2 over time. Performance begins to plateau after the sixth round, which we hypothesize is due to model performance limitations. Appendix E provides additional evaluation on a static, held-out set of human demonstration data.

⁹Accuracy is estimated by annotating 800 instructions per round.

Influence of User Adaptation on Performance

User adaptation over time is a confounding factor, because improvements in agent performance may be due to users adapting what tasks they delegate to the follower agent or how they phrase their instructions. We conduct an additional deployment with both the initial agent with parameters θ_1 and the last deployed agent with parameters θ_{11} . The agents are deployed concurrently in a randomized experiment. Users do not know which agent they are collaborating with. We collect 571 interactions, with a total of 7,784 instructions. Points on the righthand side of Figure 2 show the performance of both models during this deployment. Execution accuracy for the initial model θ_1 improves from an average of 66.7 to 70.4 from user adaptation alone, while the final agent achieves an accuracy rate of 83.6 during this side-by-side comparison.¹⁰ This demonstrates that while roughly 20% of the improvement is due to user adaptation, genuine agent improvement through continual learning is extremely effective.

User Perception of Agent Behavior User perception of the agent improves over time, as indicated by improvements in in-game feedback (Figure 3): the rate of positive feedback per action increases from 44.9 to 60.3% and the rate of negative feedback decreases from 10.1 to 4.7%. The reboot rate per instruction also decreases from 15.2 to 8.7%. After each interaction, we ask the leader for their agreement with several statements about the follower. Figure 4 shows the distribution of these post-interaction Likert ratings, which improve significantly over the 11 rounds.

Error Analysis Table 1 shows the trends of seven error types for the agent across rounds in the long-term experiment.¹¹ All but one error type decreases significantly over time, while the rate of inefficient executions remains stable (Error 6). A manual analysis shows that more than a third of remaining missed-card errors (Error 1) could be attributed to poorly-written instructions, while most extra-card errors (Error 2) occur when the incorrect card shares at least one property with the target, or is closer to the starting position than the target.

¹⁰Accuracy is estimated by annotating 400 executed instructions per agent for these additional interactions.

¹¹Error categorization is done as part of our accuracy estimation using 800 executed instructions per round.

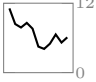



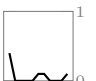
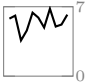

Error	$\rho = 1$	$\rho = 11$	Trend
1 Missed card Missed a card that should have been selected.	11.1	6.1	
2 Extra card Selected a card that should not have been selected.	11.4	4.6	
3 Wrong stop Stopped in the wrong position.	4.5	2.1	
4 Wrong turn Turned the wrong way when told to go left, right, backward, etc.	2.6	1.3	
5 Wrong order Accomplished the right tasks, but in the wrong order.	0.6	0.1	
6 Inefficient The follower took unnecessary, extra, or redundant steps.	5.8	6.3	
7 Other	1.1	0.4	

Table 1: Instruction execution errors during 11 rounds for seven common categories. The center columns show the prevalence of each error type as a proportion of analyzed instructions, for the initial ($\rho = 1$) and final ($\rho = 11$) agents. The rightmost column shows the trend in prevalence over time.

Language Change Users are likely to change their language over time, as observed in human-human interactions in CEREALBAR (Effenberger et al., 2021). In our study, instruction length remains relatively stable over time at an average of 8.6 tokens per utterance. We observe changes in instruction content over time, using heuristics to estimate the number of target cards specified in each instruction. There is a decrease in the rate of instructions that specify no cards to interact with (i.e., cards to select or deselect) from 12.0 in the first round to 7.7% in the last. The rate of instructions specifying a single card increases from 81.5 to 88.7%, while the rate of instructions specifying multiple cards decreases from 6.5 to 3.7%. This is potentially because no-card instructions are relatively inefficient, while multi-card instructions are relatively hard and have a higher risk of cascading errors that require corrections (i.e., deselecting a wrongly selected card). We also find that the rate of instructions containing a reference to an object (e.g., a tree, a pond) decreases over time from 17.9 to 13.5% of instructions. These changes illustrate the impact of users developing game strategies and,

potentially, a model of the follower’s instruction following ability.

5.2 Comparison of Learning Design Choices

We conduct a second deployment experiment to study the impact of the amount of initial demonstration data, negative feedback, and reward propagation heuristics. We also compare the feedback learning signal to supervised demonstration data. We design and deploy five system variations:

REWARDPROP uses the exactly same process as in the long-term experiment (Section 5.1), including reward propagation (Section 3.2).

SIMPLEREWARD measures the effect densifying and de-noising user feedback with heuristics by using only the simple reward (Section 3.2).

NONNEGATIVE simulates using positive feedback only. We discard all negative feedback, including reboots, from the data, and then apply the reward propagation heuristics (Section 3.2).¹²

FEWERDEMO uses only 144 human-human interactions (2,114 instructions) for initialization, about 25% of the supervised data used in REWARDPROP.

SUPONLY compares training with human demonstrations vs. feedback data given the same number of interactions. SUPONLY does not use data from the human-agent interactions, even though we deploy it for evaluation. Instead, after each round, we add a fixed number of additional human-human interactions to the training set, equivalent to the amount of data collected with the other variants. Due to the limited amount of demonstration data, we are only able to deploy this approach for three rounds.

We deploy the five variations for five rounds. In each rounds, all variations are deployed concurrently, each for 200 user interactions. To ensure that each worker interacts with all agents and to reduce ordering bias, we assign each worker a unique, consistent, and random ordering of agents; as they play multiple games, they cycle through agents in this order.¹³ Because all variants except FEWERDEMO are trained on the same initial data, we

¹²We do not remove the option to provide negative feedback during games in this experiment. Leaders are not informed that negative feedback will be discarded for training. We leave the direct comparison between positive-only and positive-and-negative user interfaces for future work.

¹³If we get more than 200 interactions per round because of the crowdsourcing process, we select exactly 200 games

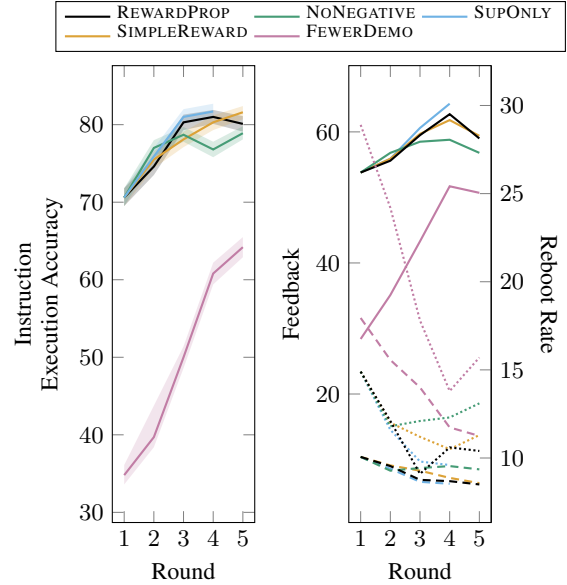


Figure 5: Results for five agent variants over five rounds. Left: mean estimated instruction execution accuracy. Right: rate of positive (✓) and negative (✗) feedback, and instruction reboot rate (↻).

deploy a single agent for all but FEWERDEMO in the first round. This experiment cost \$16,769.46.

Figure 5 shows results for the five agent variants over five rounds. Overall, learning from feedback is robust to the different design choices.¹⁴ Reward propagation (REWARDPROP) has minor benefit relative to the simple reward (SIMPLEREWARD). REWARDPROP shows slightly faster learning, which means SIMPLEREWARD gives a poorer user experience early on, even though it catches up quickly.

We observe that negative feedback is important: compared to REWARDPROP and SIMPLEREWARD, NONNEGATIVE learns slower, receives less positive feedback, and more negative feedback and reboots. This difference does not show in early rounds, but only appears around round three. It particularly stands out in the fourth round, when NONNEGATIVE shows an accuracy of 76.8 ± 1.0 , compared to 81.0 ± 0.9 of REWARDPROP.

The experiment illustrates that we can likely start with a much weaker agent. FEWERDEMO uses roughly a quarter of the demonstration initialization data available to the other variants, and indeed starts with much lower performance, 34.8 ± 1.8 accuracy, compared to 70.6 ± 1.1 for the others. Even this weak model is sufficient for effective

for training and analysis by preferring earlier games played by each worker. We discard the other games.

¹⁴The agreement of users with post-interaction statements follows similar trends. We visualize it in Section E.1.

learning. The weaker starting points leads to a much steeper learning curve, and FEWERDEMO improves to 64.2 ± 1.5 accuracy after five rounds. However, this comes at cost to the initial user experience: in the first round, only 2% of interactions with FEWERDEMO were rated positively by users.

Finally, we observe the feedback data is roughly equivalent to supervised data as a learning signal, showing similar accuracy and feedback trends, with a very slight advantage to supervised data. Overall, REWARDPROP achieves equivalent performance to SUPONLY with less than half the amount of demonstration data (i.e., as used for initialization). This shows the benefits of training through user interaction: not only are learning signals directly targeting current agent behavior, but the training process is significantly less expensive.

6 Related Work

Learning for instruction following commonly relies on data with varying levels of supervision, such as gold-standard human demonstrations (e.g., [Chen and Mooney, 2011](#); [Tellex et al., 2011](#); [Duvall et al., 2013](#); [Misra et al., 2017](#); [Anderson et al., 2018](#); [Blukis et al., 2018a,b](#); [Suhr et al., 2019](#); [Chen et al., 2019](#); [Shridhar et al., 2020](#)), or goal annotations (e.g., [Artzi and Zettlemoyer, 2013](#); [Misra et al., 2018](#); [Suhr et al., 2018](#)). We collapse the distinction between learning and deployment, shifting both training and evaluation into human-agent interactions, relying only on a small amount of human demonstration data to kickstart the process.

There has been limited work on continual learning for language-related tasks. The most technically related work to ours is [Kojima et al. \(2021\)](#), who focuses on instruction generation and continual learning using implicit feedback. Similar to this work and the machine translation work of [Kreutzer et al. \(2018a,b\)](#), we cast learning as a contextual bandit problem. Human feedback through annotation or selection of intended output was studied for semantic parsing ([Wang et al., 2016](#); [Iyer et al., 2017](#)) and summarization ([Stiennon et al., 2020](#)). This is related to soliciting partial annotations through dialogue ([Artzi and Zettlemoyer, 2011](#); [Thomason et al., 2015](#); [Yao et al., 2020](#)). Post-interaction feedback was studied in the context of dialogue ([Liu et al., 2018](#)). In contrast to existing work, we focus on sequential execution of instructions with realtime feedback.

We use the collaborative CEREALBAR sce-

nario ([Suhr et al., 2019](#)), where the user and the agent both act in the world and coordinate using natural language. Existing work with collaborative focus has primarily focused on reference games ([Krauss and Weinheimer, 1964, 1966](#); [Clark and Wilkes-Gibbs, 1986](#); [Hawkins et al., 2017](#); [Udagawa and Aizawa, 2019](#)). We focus on dynamic environments and instructional language. CEREALBAR is related to the collaborative Cards environment ([Djalali et al., 2011, 2012](#); [Potts, 2012](#)), which was used for linguistic analysis.

Continual learning through human-agent interaction has been studied more extensively outside of a language context. Our work is inspired by TAMER ([Knox and Stone, 2009](#); [Knox et al., 2013](#); [Warnell et al., 2018](#)) and COACH ([MacGlashan et al., 2017](#); [Arumugam et al., 2018](#)), where humans provide binary feedback to an agent acting in a world. While these methods were developed in the context of an agent learning a single task, we focus on generalization to previously unseen tasks specified by natural language in new environments.

7 Discussion

We propose an approach for continually learning to follow instructions through interaction with human users that provide realtime feedback. We demonstrate its effectiveness through multiple rounds of training and deployment, including thousands of interactions. We experiment with various learning design decisions, showing the learning signal and our approach are robust, and can even start from a very weak initial agent.

Our work sets the stage for several avenues of further study. There is significant potential for learning from implicit signals that do not require any additional effort from users, such as [Kojima et al. \(2021\)](#) shows for instruction generation. Such signals can supplement our explicit feedback signals. Another promising avenue for research is more expressive feedback mechanisms, such as through natural language and even complete bi-directional dialogue. Although reasoning about such signals significantly complicates both reasoning and learning, they are also much more informative. A potential direction is to use simple feedback signals like ours to bootstrap the language capabilities of the system, and then gradually switch to more complex natural language feedback.

Acknowledgments

This research was supported by ARO W911NF21-1-0106, NSF under grant No. 1750499, and a gift from Open Philanthropy. Suhr was supported by the NSF under grant No. DGE-2139899, and via a Facebook PhD Fellowship. We thank Noriyuki Kojima for discussions and sharing code, Suyi Diao for contributing to the CEREALBAR implementation, and the participating MTurk workers for their work and help in refining the user experience.

References

- Peter Anderson, Qi Wu, Damien Teney, Jake Bruce, Mark Johnson, Niko Sünderhauf, Ian Reid, Stephen Gould, and Anton van den Hengel. 2018. Vision-and-language navigation: Interpreting visually-grounded navigation instructions in real environments. In *The IEEE Conference on Computer Vision and Pattern Recognition*, pages 3674–3683.
- Yoav Artzi and Luke Zettlemoyer. 2011. [Bootstrapping semantic parsers from conversations](#). In *Proceedings of the Conference on Empirical Methods in Natural Language Processing*, pages 421–432.
- Yoav Artzi and Luke Zettlemoyer. 2013. [Weakly supervised learning of semantic parsers for mapping instructions to actions](#). *Transactions of the Association of Computational Linguistics*, 1:49–62.
- Dilip Arumugam, Jun Ki Lee, Sophie Saskin, and Michael L. Littman. 2018. Deep reinforcement learning from policy-dependent human feedback. *ArXiv*, abs/1902.04257.
- Valts Blukis, Nataly Brukhim, Andrew Bennett, Ross A. Knepper, and Yoav Artzi. 2018a. Following high-level navigation instructions on a simulated quadcopter with imitation learning. In *Proceedings of the Robotics: Science and Systems Conference*.
- Valts Blukis, Dipendra Misra, Ross A. Knepper, and Yoav Artzi. 2018b. Mapping navigation instructions to continuous control actions with position visitation prediction. In *Proceedings of the Conference on Robot Learning*.
- David L. Chen and Raymond J. Mooney. 2011. Learning to interpret natural language navigation instructions from observations. In *Proceedings of the National Conference on Artificial Intelligence*.
- Howard Chen, Alane Suhr, Dipendra Misra, Noah Snaveley, and Yoav Artzi. 2019. Touchdown: Natural language navigation and spatial reasoning in visual street environments. In *IEEE Conference on Computer Vision and Pattern Recognition*.
- Herbert H Clark and Deanna Wilkes-Gibbs. 1986. Referring as a collaborative process. *Cognition*, 22(1):1–39.
- Alex Djalali, David Clausen, Sven Lauer, Karl Schultz, and Christopher Potts. 2011. Modeling expert effects and common ground using questions under discussion. In *AAAI Fall Symposium: Building Representations of Common Ground with Intelligent Agents*.
- Alex Djalali, Sven Lauer, and Christopher Potts. 2012. Corpus evidence for preference-driven interpretation. In *Logic, Language and Meaning*, pages 150–159.
- Felix Duvallet, Thomas Kollar, and Anthony Stentz. 2013. Imitation learning for natural language direction following through unknown environments. In *IEEE International Conference on Robotics and Automation*, pages 1047–1053.
- Anna Effnerberger, Rhia Singh, Eva Yan, Alane Suhr, and Yoav Artzi. 2021. [Analysis of language change in collaborative instruction following](#). In *Findings of the Association for Computational Linguistics: EMNLP 2021*, pages 2803–2811.
- Ge Gao, Eunsol Choi, and Yoav Artzi. 2022. [Simulating bandit learning from user feedback for extractive question answering](#). In *Proceedings of the Annual Meeting of the Association for Computational Linguistics*, pages 5167–5179.
- Robert X. D. Hawkins, Mike Frank, and Noah D. Goodman. 2017. Convention-formation in iterated reference games. In *Cognitive Science*.
- Sepp Hochreiter and Jürgen Schmidhuber. 1997. Long short-term memory. *Neural computation*, 9.
- Emiel Hoogeboom, Jorn W.T. Peters, Taco S. Cohen, and Max Welling. 2018. [HexaConv](#). In *International Conference on Learning Representations*.
- D. G. Horvitz and D. J. Thompson. 1952. [A generalization of sampling without replacement from a finite universe](#). *Journal of the American Statistical Association*, 47(260):663–685.
- Srinivasan Iyer, Ioannis Konstas, Alvin Cheung, Jayant Krishnamurthy, and Luke Zettlemoyer. 2017. [Learning a neural semantic parser from user feedback](#). In *Proceedings of the Annual Meeting of the Association for Computational Linguistics*, pages 963–973.
- Diederik Kingma and Jimmy Ba. 2014. Adam: A method for stochastic optimization. In *Proceedings of the International Conference on Learning Representations*.
- W. Bradley Knox and Peter Stone. 2009. Interactively shaping agents via human reinforcement: the TAMER framework. In *Proceedings of the International Conference on Knowledge Capture*.
- W. Bradley Knox, Peter Stone, and Cynthia Breazeal. 2013. Training a robot via human feedback: A case study. In *Proceedings of the International Conference on Social Robotics*.

- Noriyuki Kojima, Alane Suhr, and Yoav Artzi. 2021. [Continual learning for grounded instruction generation by observing human following behavior](#). *Transactions of the Association for Computational Linguistics*, 9:1303–1319.
- Robert M. Krauss and Sidney Weinheimer. 1964. Changes in reference phrases as a function of frequency of usage in social interaction: a preliminary study. *Psychonomic Science*, 1:113–114.
- Robert M. Krauss and Sidney Weinheimer. 1966. Concurrent feedback, confirmation, and the encoding of referents in verbal communication. *Journal of personality and social psychology*, 4 3:343–6.
- Julia Kreutzer, Shahram Khadivi, Evgeny Matusov, and Stefan Riezler. 2018a. [Can neural machine translation be improved with user feedback?](#) In *Proceedings of the Conference of the North American Chapter of the Association for Computational Linguistics: Human Language Technologies*, pages 92–105.
- Julia Kreutzer, Joshua Uyheng, and Stefan Riezler. 2018b. [Reliability and learnability of human bandit feedback for sequence-to-sequence reinforcement learning](#). In *Proceedings of the Annual Meeting of the Association for Computational Linguistics*, pages 1777–1788.
- Bing Liu, Gokhan Tür, Dilek Hakkani-Tür, Pararth Shah, and Larry Heck. 2018. [Dialogue learning with human teaching and feedback in end-to-end trainable task-oriented dialogue systems](#). In *Proceedings of the Conference of the North American Chapter of the Association for Computational Linguistics: Human Language Technologies*, pages 2060–2069.
- James MacGlashan, Mark K. Ho, Robert Tyler Loftin, Bei Peng, David L. Roberts, Matthew E. Taylor, and Michael L. Littman. 2017. Interactive learning from policy-dependent human feedback. In *Proceedings of the International Conference on Machine Learning*.
- Dipendra Misra, Andrew Bennett, Valts Blukis, Eyvind Niklasson, Max Shatkhin, and Yoav Artzi. 2018. [Mapping instructions to actions in 3D environments with visual goal prediction](#). In *Proceedings of the Conference on Empirical Methods in Natural Language Processing*, pages 2667–2678.
- Dipendra Misra, John Langford, and Yoav Artzi. 2017. [Mapping instructions and visual observations to actions with reinforcement learning](#). In *Proceedings of the Conference on Empirical Methods in Natural Language Processing*, pages 1004–1015.
- Christopher Potts. 2012. Goal-driven answers in the Cards dialogue corpus. In *Proceedings of the West Coast Conference on Formal Linguistics*, pages 1–20.
- Rico Sennrich, Barry Haddow, and Alexandra Birch. 2016. [Neural machine translation of rare words with subword units](#). In *Proceedings of the Annual Meeting of the Association for Computational Linguistics*, pages 1715–1725.
- Mohit Shridhar, Jesse Thomason, Daniel Gordon, Yonatan Bisk, Winson Han, Roozbeh Mottaghi, Luke Zettlemoyer, and Dieter Fox. 2020. ALFRED: A benchmark for interpreting grounded instructions for everyday tasks. In *IEEE Conference on Computer Vision and Pattern Recognition*.
- Nisan Stiennon, Long Ouyang, Jeffrey Wu, Daniel Ziegler, Ryan Lowe, Chelsea Voss, Alec Radford, Dario Amodei, and Paul F. Christiano. 2020. [Learning to summarize with human feedback](#). In *Advances in Neural Information Processing Systems*, volume 33, pages 3008–3021.
- Alane Suhr, Srinivasan Iyer, and Yoav Artzi. 2018. [Learning to map context-dependent sentences to executable formal queries](#). In *Proceedings of the Conference of the North American Chapter of the Association for Computational Linguistics: Human Language Technologies*, pages 2238–2249.
- Alane Suhr, Claudia Yan, Charlotte Schluger, Stanley Yu, Hadi Khader, Marwa Mouallem, Iris Zhang, and Yoav Artzi. 2019. [Executing instructions in situated collaborative interactions](#). In *Proceedings of the Conference on Empirical Methods in Natural Language Processing*.
- Richard S. Sutton and Andrew G. Barto. 1998. Reinforcement learning: An introduction. *IEEE Transactions on Neural Networks*, 9:1054–1054.
- Stephanie Tellex, Thomas Kollar, Steven Dickerson, Matthew R. Walter, Ashis Gopal Banerjee, Seth Teller, and Nicholas Roy. 2011. Understanding natural language commands for robotic navigation and mobile manipulation. In *Proceedings of the National Conference on Artificial Intelligence*.
- Jesse Thomason, Shiqi Zhang, Raymond Mooney, and Peter Stone. 2015. Learning to interpret natural language commands through human-robot dialog. In *Proceedings of the International Joint Conference on Artificial Intelligence*.
- Takuma Udagawa and Akiko Aizawa. 2019. A natural language corpus of common grounding under continuous and partially-observable context. In *Proceedings of the Conference on Artificial Intelligence*.
- Sida I. Wang, Percy Liang, and Christopher D. Manning. 2016. [Learning language games through interaction](#). In *Proceedings of the Annual Meeting of the Association for Computational Linguistics*, pages 2368–2378.
- Garrett Warnell, Nicholas R. Waytowich, Vernon Lawhern, and Peter R Stone. 2018. Deep TAMER: Interactive agent shaping in high-dimensional state spaces. In *Proceedings of the Conference on Artificial Intelligence*.

Ziyu Yao, Yiqi Tang, Wen-tau Yih, Huan Sun, and Yu Su. 2020. [An imitation game for learning semantic parsers from user interaction](#). In *Proceedings of the Conference on Empirical Methods in Natural Language Processing*, pages 6883–6902.

A Model

We implement our policy as a neural network based on the design of [Suhr et al. \(2019\)](#). The inputs are an instruction \bar{x} and observation o , and the output is a distribution over actions. The policy architecture is composed of several modules that combine to a single network.

Embedding Instructions We embed the instruction $\bar{x} = \langle x_1, \dots, x_n \rangle$ of length n with a bidirectional recurrent LSTM ([Hochreiter and Schmidhuber, 1997](#)). This results in a sequence of hidden states $\langle \mathbf{h}_1, \dots, \mathbf{h}_n \rangle$. The embedding of \bar{x} is the final hidden state of the sequence \mathbf{h}_n .

Embedding Observations Each agent observation o includes information about the observable environment and the instruction execution so far. The follower agent in CEREALBAR has partial observability. We use a representation similar to that of [Suhr et al. \(2019\)](#), but without making the simplifying assumption of full observability. The environment state \mathbf{W} is a tensor representing the properties of each position in the environment as embedding indices. The properties represented in \mathbf{W} also encode information about the follower’s trajectory so far, the presence of obstacles in the environment, and the follower’s observability. Due to partial observability, each position’s representation is derived from its most recent observation; any information that changes about the world may be outdated in \mathbf{W} . We embed \mathbf{W} into a dense tensor \mathbf{W}' .

Fusing Embeddings After independently embedding the instruction and observation into \mathbf{h}_n and \mathbf{W}' , we compute a joint representation of both inputs using text-conditioned (i.e., via \mathbf{h}_n) convolutions over \mathbf{W}' .

Transforming the Coordinate System Predicting actions requires interactions between representations of multiple positions. \mathbf{W}' represents the environment using offset coordinates, which do not precisely represent the structure of hexagonal grid in CEREALBAR. We transform \mathbf{W}' to axial coordinates ([Hoogeboom et al., 2018](#)), and translate and rotate the tensor such that the center position represents the agent’s current location, and the agent is facing in a consistent direction. These transformations are not parameterized.

LINGUNET We use LINGUNET ([Blukis et al., 2018b](#)) to predict the policy distribution over actions $\pi(\cdot \mid \bar{x}, o; \theta)$, with slight modifications to the

design of [Suhr et al. \(2019\)](#). For all convolutions, we apply hex-based convolutions with kernels that operate only on voxels within a hex diameter of d around the center voxel, for a kernel size of d . We apply instance normalization to the last LINGUNET layer of the input and text-based convolutions. Finally, we do not perform the final transposed convolution. Instead, we directly predict a distribution over the action space given the output of the transposed convolution.

A.1 Inference

We use ensemble-based inference. Given sets of model parameters $\theta = \langle \theta_1, \dots, \theta_m \rangle$, we construct a policy π over executable actions using voting:¹⁵

$$\pi(a \mid \bar{x}, o; \theta) \propto \exp \left(\sum_{1 \leq i \leq m} \mathbb{1}_{a = \arg \max \pi(\cdot \mid \bar{x}, o; \theta_i)} \right).$$

Actions are sampled and executed from $\pi(\cdot \mid \bar{x}, o; \theta)$. Executing an action in the environment results in a observation according to the transition function \mathcal{T} . We continue to sample actions until the stop action STOP is sampled, or until the leader manually reboots the follower. The STOP action marks the current instruction as complete, which either results in the follower’s turn ending, or it receiving the next instruction to follow.

B Implementation Details

We lowercase and tokenize instructions using BPE ([Sennrich et al., 2016](#)) with a maximum vocabulary size of 4,096 and a minimum wordtype occurrence of 2.¹⁶ We learn size-64 word embeddings from scratch. We encode instructions with a single-layer LSTM RNN ([Hochreiter and Schmidhuber, 1997](#)) with 128 hidden units. We embed each position’s properties into vectors of size 16. We use the same LINGUNET hyperparameters as [Suhr et al. \(2019\)](#).

We use an ensemble size of $m = 10$. We do not train in ensemble, but train ten separate models and apply ensemble-based inference during deployment. When using reward propagation, we use a maximum distance of 8 for propagating to previous actions that received no feedback. For training, we use a batch size of 16 agent steps, a learning rate of

¹⁵We assign zero probability to inexecutable actions, i.e., one that would result in an intersection with an obstacle.

¹⁶We use the implementation provided by HuggingFace at <https://huggingface.co/docs/tokenizers/>.

0.001, and ADAM (Kingma and Ba, 2014) for optimization. We re-initialize model parameters from scratch at the beginning of each round of parameter optimization. We use a held-out subset of the original CEREALBAR training set as a validation set for early stopping, comprising 5% of the original split. After each epoch, we evaluate model performance using SWSD (Appendix C) on the validation set, and use patience for model selection.

C Evaluation

Instruction Execution Accuracy For each deployed agent, we randomly sample instruction execution traces $\mathcal{E}_e \subseteq \mathcal{E}_c \subseteq \mathcal{E}$ for manual evaluation. \mathcal{E}_c contains all instructions marked as complete by the agent, and \mathcal{E} contains instructions that were either marked as complete or rebooted.¹⁷ Excluding rebooted instructions from this evaluation creates a biased sample, as reboots nearly always reflect incorrect instruction execution, so we re-adjust accuracy estimates based on reboot rates. We assume all rebooted instructions are incorrect executions. The adjusted correctness rate is:

$$\text{correctness} = \frac{\sum_{\bar{e} \in \mathcal{E}_e} \mathbb{1}_{\text{correct}(\bar{x}, \bar{e})} |\mathcal{E}_c|}{|\mathcal{E}_e| |\mathcal{E}|},$$

where $\text{correct}(\bar{x}, \bar{e})$ is user judgment of execution $\bar{e} = \langle (o_i, a_i, w_i^a) \rangle_{i=1}^m$ for instruction \bar{x} .

Static Evaluation Data We also evaluate on the development split from Suhr et al. (2019), with *success weighted by stopping distance* (SWSD). SWSD is computed per instruction execution:

$$\text{SWSD}(\bar{e}', \bar{e}^*) = \frac{\mathbb{1}_{\bar{e}'_{-1} \equiv \bar{e}^*_{-1}}}{1 + \|\bar{e}'_{-1} - \bar{e}^*_{-1}\|},$$

where \bar{e}' is the trace of the agent’s execution of an instruction and \bar{e}^* is the human demonstration. $\bar{e}'_{-1} \equiv \bar{e}^*_{-1}$ only if \bar{e}' results in the same set of cards selected as in \bar{e}^* . $\|\bar{e}'_{-1} - \bar{e}^*_{-1}\|$ is the hex distance between stopping positions. SWSD is stricter than simple card-state accuracy (Suhr et al., 2019), as it gives only partial credit to instructions where an execution stops in an incorrect position.

D Crowdsourcing Details

We qualify workers through a tutorial and a short quiz about the game rules. Workers are also required to reside in an English-majority locale and

have a HIT approval rate of over 90% with at least 100 approved HITs during their time on MTurk. The base pay for completing the qualification task is \$0.50 USD, and qualified workers receive a \$2.00 bonus. We qualify 108 workers. Following Suhr et al. (2019), we pay workers bonuses per point earned in each game, increasing the compensation per point as the game score increases. On average across all experiments, each game costs \$2.91 and workers are paid an average of \$21.85 per hour.

We split workers into two pools: expert and novice. Expert workers earn a 50% higher bonus per game than novice workers. Workers are moved to the expert pool after playing at least two games with a score greater than zero, as long as their rate of giving feedback is greater than 75% of instructions.¹⁸ Workers return to the novice pool if they play for two rounds with a feedback rate of less than 75% of instructions. 65 workers achieve and maintain expert status throughout the experiments. Only expert workers are qualified to provide post-hoc instruction execution judgments, where they are paid \$0.07 per judgment of instruction execution.

E Additional Results

E.1 User Perception of Agents for Comparison of Learning Design Choices

Figure 6 shows the Likert distribution for the three post-interaction statements users are asked about for the experiments comparing learning design choices, where we concurrently deployed five systems for five rounds.

E.2 Evaluation on Static Data

Evaluation through human-agent interaction is the main focus of our work. However, we also evaluate instruction-following agents against held-out, static data from Suhr et al. (2019). This evaluation does not take into account how the actual data distribution shifts over the agent’s lifetime, because of the dynamics between the agent and human users. Figure 7 shows average SWSD for the models deployed in each round. SWSD begins at 39.7 for the initial model, and peaks at 46.4. This improvement is due entirely to adding training data acquired from human-agent interactions.

¹⁷In this evaluation, we ignore all instructions that were not completed due to the game ending.

¹⁸The rate of feedback per instruction measures the proportion of instructions where at least one action in the follower’s instruction execution is given positive or negative feedback, including a reboot.

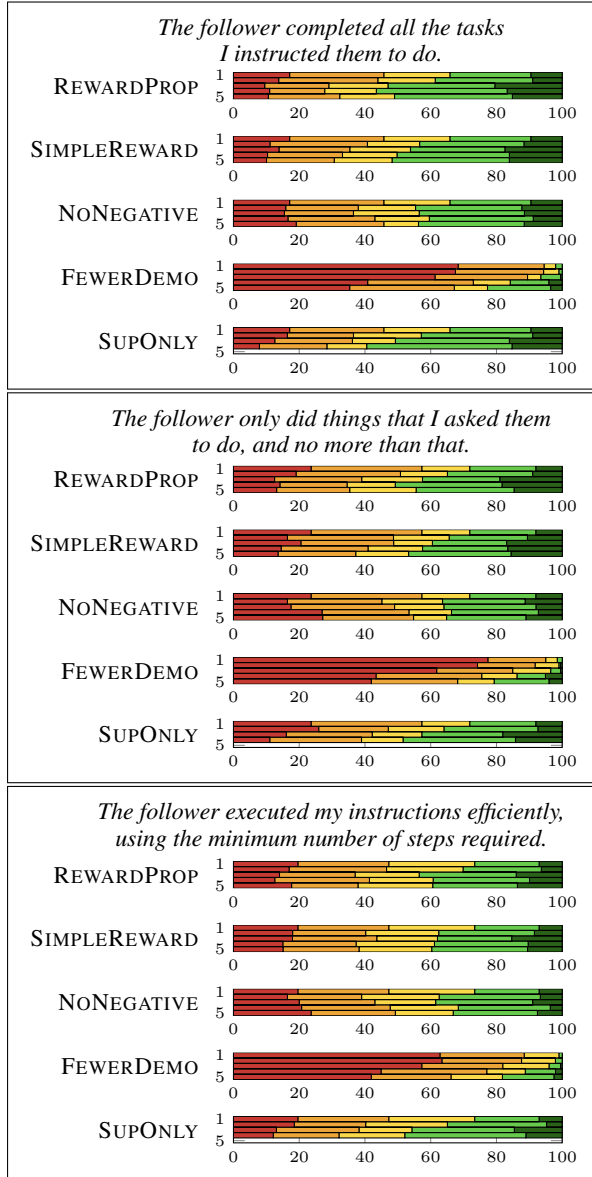


Figure 6: Distribution of post-interaction user agreement with three statements about the follower’s performance for our approach comparison experiment.

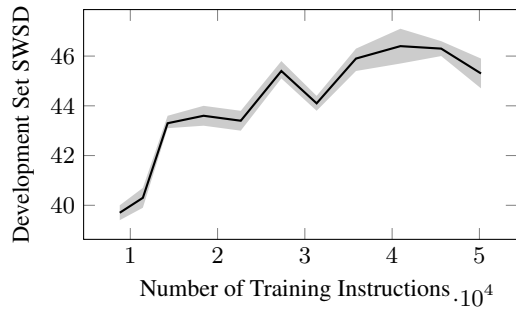


Figure 7: SWSD on the held-out development data, averaged over five runs of sampling-based inference.